IOP PUBLISHING METROLOGIA
Metrologia **46** (2009) 416–422 doi:10.1088/0026-1394/46/5/005

The coefficient of thermal expansion of highly enriched ^{28}Si

Guido Bartl[1], Arnold Nicolaus[1], Ernest Kessler[2], René Schödel[1] and Peter Becker[1]

[1] Physikalisch-Technische Bundesanstalt (PTB), Bundesallee 100, D-38116 Braunschweig, Germany
[2] National Institute of Standards and Technology (NIST), Gaithersburg, MD 20899 USA

Received 8 April 2009, in final form 20 May 2009
Published 24 June 2009
Online at stacks.iop.org/Met/46/416

Abstract
For the new definition of the SI unit of mass based on a fundamental constant, a redetermination of Avogadro's constant is the goal of an international collaboration of numerous national laboratories and universities. Since a relative uncertainty of about 2×10^{-8} is aimed at, the macroscopic density, the isotopic composition and the volume of the unit cell of a silicon single crystal have to be measured with high precision. One step to improve the precision was the production of a silicon crystal of highly enriched ^{28}Si. This paper addresses the effect of thermal expansion of that material in order to account for a possible discrepancy between the coefficient of thermal expansion (CTE) of natural silicon and that of ^{28}Si. The results of two independent CTE measuring methods are presented and compared in this paper.

1. Introduction

Almost all the base units of the International System of Units (SI) have been defined by atomic constants or fundamental constants of physics. Only the kilogram is still represented by a prototype, the international kilogram prototype. For a long time now, experiments to also link the kilogram to fundamental constants have been running worldwide [1]. Metrologists of numerous national laboratories and universities have taken an important step forward with their so-called Avogadro experiment.

The presupposed final measuring uncertainty of about 2×10^{-8} to the application of the Avogadro constant in a new definition of the mass unit is a challenge for the experimental determination of all quantities involved: macroscopic density, isotopic composition and unit cell volume of a silicon crystal. A value of the Avogadro constant with a relative measurement uncertainty of 3×10^{-7} has been obtained by using single crystals of silicon with a natural isotopic composition [2]. For the final result all measured quantities have to be referred to a common temperature, e.g. 20 °C, which needs a precise knowledge of the coefficient of thermal expansion (CTE) of silicon. But the overall uncertainty attained was close to a practical limit.

To achieve a further reduction in the uncertainty of N_A, an improvement in the molar mass determination was demanded. This could be realized by fabricating an isotopically pure silicon single crystal of $\geqslant$99.99% enriched ^{28}Si [3], which means ^{29}Si and ^{30}Si abundances of the order of only 0.005%, resulting in (very) small corrections to the molar mass value of ^{28}Si, known to a relative combined uncertainty of $\leqslant 10^{-9}$. These corrections will be directly measured.

This concept has become feasible because of a source of very highly enriched Si isotopes in Nizhny Novgorod. The Institute of Chemistry of High-Purity Substances RAS (IChHPS RAS) demonstrated its capability to produce ^{28}Si with the necessary enrichment. The second step was to scale up the production facility of the Central Design Bureau of Machine Building in Saint Petersburg to produce a sufficient amount of enriched ^{28}Si in order to grow a 5 kg single crystal, which was produced in 2007 by the Institute for Crystal Growth (IKZ) in Berlin with sufficient chemical and isotopic purity. More recently, in Sydney, Australia, the Division of Industrial Physics of the CSIRO has polished two almost perfect 1 kg silicon spheres from the enriched material, which have been under investigation worldwide in the international Avogadro experiment since April 2008. With respect to the new material all quantities related to the Avogadro constant have to be remeasured with lower measurement uncertainty, and also the CTE for the enriched material was subjected to inspection. Two independent experimental approaches were therefore performed: temperature-dependent length measurements of the diameter of a macroscopic silicon sphere made of ^{28}Si and measurements of the temperature-dependent lattice parameter

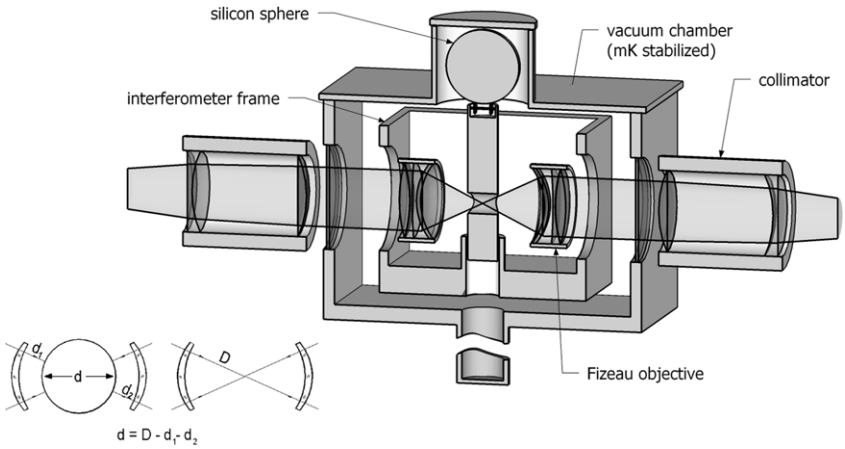

Figure 1. Experimental setup of the sphere interferometer.

changes in the microscopic domain. How much the value of the CTE of ^{28}Si differs from that of naturally composed silicon is described in the following.

2. Length change measurements with the sphere interferometer of PTB

2.1. Experimental setup

The interferometer for spheres (figure 1) has been developed at PTB for the determination of the diameter of silicon spheres for the Avogadro project [4]. The centre of the setup is defined by the sphere under test resting on a three-point support, which is tightly fixed to the solid stainless steel frame. The reference faces of two Fizeau lenses, which are mounted opposite to each other in the same frame, form a spherical etalon with the sphere in the middle. This interferometer frame is located in a vacuum chamber to eliminate influences of the refractive index of air. The illuminating and imaging optics are installed symmetrically on each side of the vacuum chamber.

The diameter of the sphere is calculated from the difference of the diameter D of the empty etalon and the distances between the reference faces and the surface of the sphere d_1 and d_2 (figure 1). Therefore the sphere has to be elevated out of the etalon, which is done by a lifting mechanism below the three-point support. In the lifted position a hole in the supporting cylinder allows the diameter D of the empty etalon to be measured.

For absolute diameter determinations a precise control of the temperature is essential [5]. This control is realized by a thermostat that stabilizes the temperature of water flowing through tubes that encase the vacuum chamber of the interferometer. Due to thermal inertia of the whole setup the residual fluctuation amounts to a few millikelvin. In order to allow for the correction of remaining deviations from the targeted measurement condition (generally 20 °C) the temperature has to be measured in the domain of 1 mK. Therefore, the temperature difference between the sphere under test and a copper block inside the interferometer chamber is measured by thermocouple pairs. One bead of each pair is in resilient contact with the surface of the sphere near the three-point support and the other is attached to the copper block. This copper block acts as a reference body in thermal contact with the interferometer chamber. This temperature measurement is traced back to the ITS-90 [6] by determining the temperature of the copper block using a platinum resistance thermometer calibrated in relation to thermometric fixed point cells.

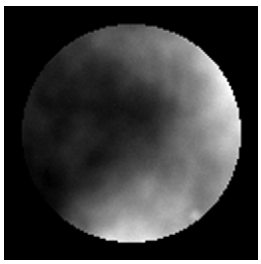

Figure 2. Topography segment of the sphere S8 inside the circular field of view of 60° at the measurement position. The greyscale spans approximately 24 nm.

2.2. Measurement procedure

For the measurement of the length of ^{28}Si as a function of the temperature two spheres made from a silicon single crystal were used as the objects under test. Each sphere was orientated to a selected position at which the diameter topography inside the field of view of the optics features only a slight slope. As an example, figure 2 displays the topography segment of sphere S8 with the greyscale corresponding to about 24 nm from peak to valley. At different stabilized temperatures with a fluctuation of only a few millikelvin series of measurements were performed with each series containing four to eleven diameter measurements. The targeted temperatures were set by the thermostat in an interval between 17.5 °C and 30.0 °C. Since the temperature changes are large compared with the thermal time constant of the interferometer, after each change a period of some days had to elapse until an acceptable equilibrium at the millikelvin level was reached again.

One single diameter measurement process provides 9856 measurement values given by the pixels of the camera. The resulting interferograms were evaluated as described in [4] so that every pixel corresponds to one value L, which is the

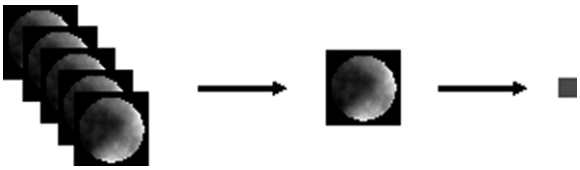

Figure 3. Principle of the averaging process of one series of measurements at a certain temperature. In the first step the topographies are averaged pixelwise. The averaged topography is then, in the second step, averaged over the field of view to yield one mean length value for the diameter.

diameter of the sphere at the respective position inside the field of view.

2.3. Evaluation of the CTE and its uncertainty

The CTE, named α, is defined as [7]

$$\alpha = \frac{1}{L}\frac{\mathrm{d}L}{\mathrm{d}T}, \tag{1}$$

where L is a continuous length as a function of the kelvin temperature. In order to generate such a continuous function from length measured at given temperatures a least square fitting procedure can be applied. For this purpose the length is described as a function of the temperature by a polynomial of degree n from which the CTE is calculated:

$$L^{(n)} = a_0 + a_1(T - T_0) + a_2(T - T_0)^2 + \cdots + a_n(T - T_0)^n,$$
$$\alpha^{(n)} = \frac{1}{L^{(n)}}\frac{\mathrm{d}L^{(n)}}{\mathrm{d}T}, \tag{2}$$

where T is the temperature in kelvin and T_0 defines a certain point within the temperature interval.

In principle, it is possible to apply the fitting to each specific length value assigned to a certain pixel position within the diameter topography. However, it is more applicable to average the diameter topographies within the entire field of view before the fitting is applied. In fact, the variation of the length within a topography is surely less than 50 nm. Accordingly, the error induced by the averaging of the diameters within the topography can be estimated to be $10^{-12}\,\mathrm{K}^{-1}$ and is thus negligible. Furthermore, sets of measurements performed at the same temperature were averaged pixelwise to reduce noise. Then, as stated before, they were averaged again over the field of view. The principle of this process is shown schematically in figure 3.

Applying a number of temperatures leads to a data set $\{\bar{t}_i, \bar{l}_i\}$, where $\bar{t}_i$ are the mean temperatures and $\bar{l}_i$ the mean of the averaged lengths. Such a data set constitutes the basis for the calculation of the CTE of ^{28}Si.

An effective method of uncertainty evaluation is the use of symbolic computation by *MATHEMATICA*® (Wolfram Research) as described in [8]. In short, the measured data points are replaced by free variables and, just in a final step, the data are inserted into the symbolic expressions. This gives the possibility to calculate derivatives of the resulting coefficients in order to extract sensitivity coefficients as required by the '*Guide to the Expression of Uncertainty in Measurement*' (GUM) [9]. The minimum of $\chi^2 = \sum_{i=1}^{N}(\bar{l}_i - L^{(n)}(\bar{t}_i))^2$,

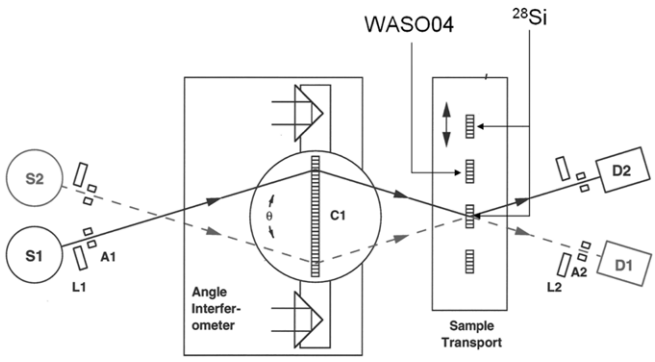

Figure 4. Setup for the comparison of the lattice parameters of ^{28}Si and $^{\mathrm{nat}}$Si crystals.

with N being the number of data points, is obtained from the algebraic solution of the set of $n+1$ equations: $(\partial/\partial a_k)(\chi^2) = 0$, $k = 0 \ldots n$, resulting in symbolic expressions for the coefficients a_k of the fitted polynomial. The uncertainties of the a_k are calculated according to

$$u(a_k) = \sqrt{\sum_{i=1}^{N}\left[\left(\frac{\partial a_k}{\partial l_i}(l_i)\right)^2 + \left(\frac{\partial a_k}{\partial t_i}u(t_i)\right)^2\right]}. \tag{3}$$

Then the uncertainty of the CTE can be obtained from

$$u(\alpha) = \sqrt{\sum_{k=0}^{n}\left(\frac{\partial \alpha}{\partial a_k}u(a_k)\right)^2}. \tag{4}$$

In a final step the measured data $\{\bar{t}_i, \bar{l}_i\}$ and their uncertainties $\{u(\bar{t}_i), u(\bar{l}_i)\}$ are inserted so that numeric expressions for a_k and $u(a_k)$ and therewith for α and $u(\alpha)$ are returned. In this approach it is useful to set T_0 in equation (2) to the centre of the overall temperature interval of interest.

The straightforward calculation of $u(\alpha)$ resulting in equation (4) presumes that the length can be described as a function of the temperature by a polynomial of certain degree n. However, the functional relationship between the length and the temperature for a given material is not known on the nanometre scale. Therefore, the choice of the polynomial degree in equation (2) is arbitrary and there is an unknown deviation of the material intrinsic thermal expansion compared with the CTE obtained. This deviation can by far exceed $u(\alpha)$ obtained from equation (4) as demonstrated in [10]. Therefore, an additional uncertainty contribution due to the arbitrariness of the fitted polynomial is considered via the expression $|\alpha^{(n+1)} - \alpha^{(n)}|$.

3. Measurements of the lattice parameter at NIST

3.1. Experimental setup

The NIST lattice comparison spectrometer measures the difference in lattice spacing of two crystal samples [11, 12]. Lattice spacing differences are inferred from the measured Bragg angles differences. The comparator uses the Laue case two-crystal geometry (figure 4) and has a translation slide that

Table 1. Length values (diameters of the ^{28}Si sphere) as a function of temperature.

Data set i	Temperature $\bar{t}_i$/°C	$u\left(\bar{t}_i\right)$/°C	Averaged length $\bar{l}_i$/mm	$u(\bar{l}_i)$/nm
1	17.588	0.001	93.721 6725	1.2
2	18.835	0.001	93.721 9686	1.0
3	19.978	0.001	93.722 2419	1.0
4	19.981	0.001	93.722 2425	0.9
5	19.997	0.001	93.722 2460	0.9
6	20.056	0.001	93.722 2601	1.0
7	21.174	0.001	93.722 5285	1.0
8	22.442	0.001	93.722 8335	1.2
9	26.044	0.001	93.723 7080	1.5
10	28.094	0.001	93.724 2109	1.5
11	29.698	0.001	93.724 6050	1.5

permits remote interchange of the crystal samples that are being compared. The Bragg angle differences are measured with a sensitive heterodyne interferometer. The first long crystal and the second crystal samples have lamellas with nearly equally thickness so that the recorded x-ray profiles exhibit Pendellosung oscillations which contribute to a more accurate determination of profile centres.

In the measurements reported here the difference in lattice spacing between a natural silicon (^{nat}Si) crystal and a ^{28}Si crystal was measured as a function of temperature. The lattice spacing difference as a function of temperature is a measure of the difference between the thermal expansion coefficients of ^{nat}Si and ^{28}Si as a function of temperature. Because only the difference of the thermal expansion coefficients of ^{nat}Si and ^{28}Si is measured and because the spectrometer is located in an environment where the temperature is not easily varied, the contribution of these measurements to a precise determination of the CTE of ^{28}Si is limited. However, these measurements do provide an important and independent confirmation of the direct and more complete CTE measurements of ^{28}Si described in section 2 above.

3.2. Measurement procedure and evaluation

For the CTE measurements a ^{nat}Si crystal from the WASO 04 boule and a ^{28}Si crystal from the ^{28}Si 5 kg single crystal produced for the Avogadro project were mounted on the translation slide. The coordinates of the ^{nat}Si crystal within the WASO 04 boule were: longitudinal 143 cm and radial near the centre of the boule. The coordinates of the ^{28}Si crystal within the 5 kg ^{28}Si boule were: longitudinal 17.4 cm to 17.9 cm and radial near the surface of the boule. The set point for the room temperature was at the nominal 20 °C which results in a stable temperature of about 21.1 °C at the second crystal position when the x-ray tubes have been continuously operating for about 24 h. The lattice spacing differences between the ^{nat}Si crystal and the long first crystal and between the ^{28}Si crystal and the long first crystal were sequentially measured in three data runs, each lasting about 24 h. By subtraction, the lattice spacing difference between ^{nat}Si and ^{28}Si was obtained for each of these runs and the results from the three runs were averaged.

Then the set point of the room was raised to 23.1 °C (maximum temperature allowed by the heating and air conditioning controls) and the room and spectrometer (with x-ray tubes operating) stabilized after 6 days to about 24.2 °C at the second crystal position. Lattice spacing differences were again measured in five data runs covering 6 days. The results were averaged.

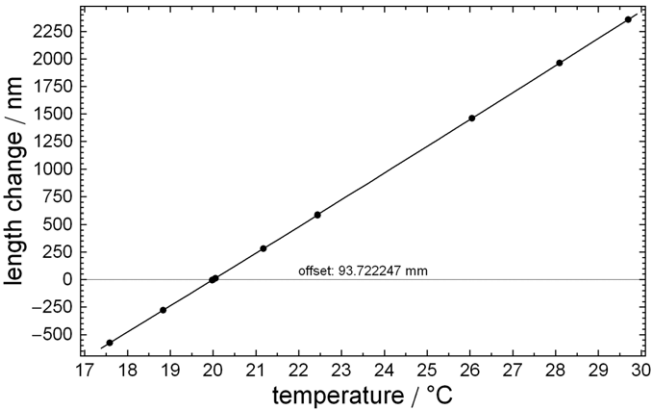

Figure 5. Change of the mean average length $\bar{l}$ in relation to the length at the reference temperature of 20 °C. The solid line is a linear fit to the measurement data.

The set point of the room was returned to 20 °C and after about 5 days the temperature at the second crystal position returned to 21.1 °C. Lattice spacing differences were measured in two data runs over 2 days and the results were averaged. Because the first and third sets were recorded at almost the same temperature, these lattice spacing difference measurements provide a check on the CTE at essentially only two temperatures.

4. Results and discussion

4.1. Results of the measurements at PTB

Following the evaluation procedure described in section 2.3, a polynomial fit according to equation (2) is applied to the mean average length values which are presented in table 1 including the temperature values and the corresponding standard uncertainties. The uncertainties of the length values for temperatures apart from 20 °C are slightly increased due to the fact that the temperature stabilization works most efficiently at 20 °C. In figure 5 the result of a fit of the degree $n = 1$ is shown together with the measurement values. Since

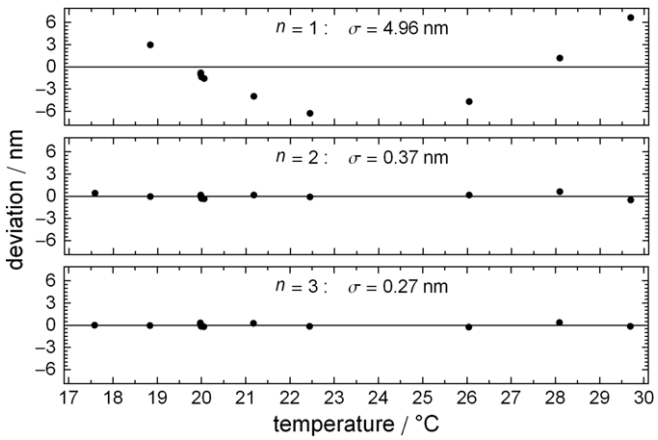

Figure 6. Deviation of the measurement data from the polynomial fits up to the degree $n = 3$.

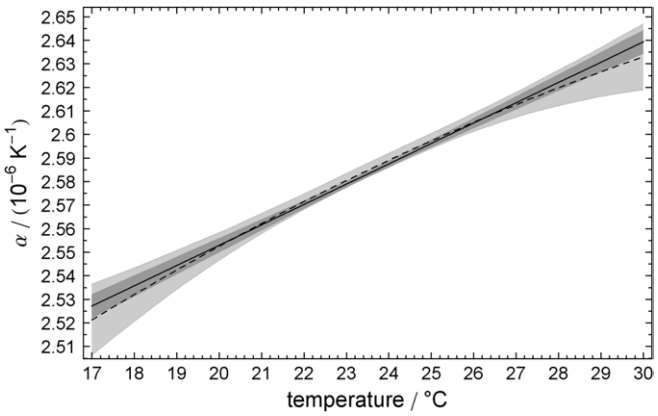

Figure 7. Results of the calculations of the CTE of ^{28}Si based on the polynomial fits of the degrees $n = 2$ (solid line) and $n = 3$ (dashed line) as a function of temperature. The dark grey area indicates the uncertainty of the case $n = 2$ and the light grey the uncertainty for $n = 3$.

this plot does not reveal the residuals, in figure 6 the deviation of the fitted polynomial from the measurement values is shown for the polynomials up to the degree $n = 3$. The standard deviation in the form

$$\sigma = \sqrt{\frac{\sum_{i=0}^{N} \left(\bar{l}_i - L^{(n)}(\vartheta_i)\right)^2}{N - (n+1)}}$$

acts as a figure of merit of the fit and takes into account the number of free parameters, which is $n + 1$ for a polynomial of degree n. As can be seen, using a polynomial of degree larger than $n = 1$ considerably reduces σ by an order of magnitude. Hence, in the following, the linear fit is disregarded.

The results of both the calculation of α corresponding to equation (2) and the uncertainty are plotted in figure 7 as a function of temperature. As the two cases, $n = 2$ and $n = 3$, coincide within the given temperature interval in consideration of the uncertainty, the quadratic polynomial was chosen for further evaluation.

When T_0 in equation (2) is set to 293.15 K (20 °C), a_0 represents the length at 20 °C and the related coefficients

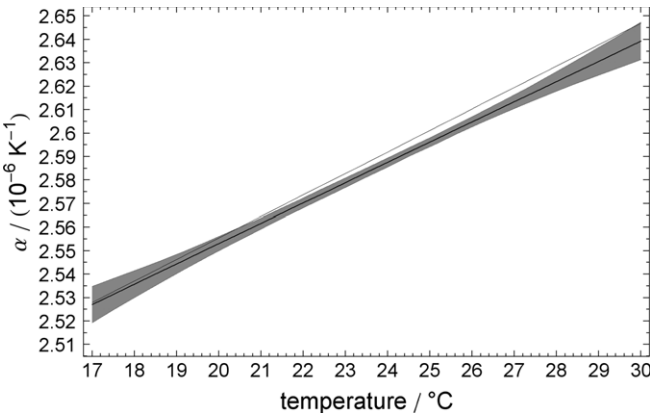

Figure 8. CTE α of ^{28}Si as a function of the temperature (heavy solid line). The dark grey area indicates the uncertainty for the case of the quadratic polynomial and additionally taking into account the difference from the cubic one. For comparison, the thin solid line is a plot of the CTE of $^{\text{nat}}$Si.

can be converted according to

$$\alpha_0 = \frac{a_1}{a_0} = 2.5530 \times 10^{-6}\,\text{K}^{-1} \pm 0.0012 \times 10^{-6}\,\text{K}^{-1} \quad \text{and}$$

$$\alpha_1 = \frac{a_2}{a_0} = 4.32 \times 10^{-9}\,\text{K}^{-2} \pm 0.37 \times 10^{-9}\,\text{K}^{-2}, \qquad (5)$$

where the uncertainty values are based on the uncertainties of the fit parameters given by equation (3).

The CTE of ^{28}Si can then be expressed as

$$\begin{aligned}\alpha_{28}(t) &= \frac{1}{L}\frac{\text{d}}{\text{d}T}L(T) \\ &= \frac{\alpha_0 + 2\,\alpha_1 \times (t - 20\,^\circ\text{C})}{1 + \alpha_0 \times (t - 20\,^\circ\text{C}) + \alpha_1 \times (t - 20\,^\circ\text{C})^2} \\ &\approx \alpha_0 + 2\,\alpha_1 \times (t - 20\,^\circ\text{C}), \qquad (6)\end{aligned}$$

in which t is the Celsius temperature ($t/^\circ\text{C} = T/\text{K} - 273.15$). Therefore, α_0 represents the value of $\alpha_{28}(t)$ at the temperature of 20 °C and the temperature dependence of $\alpha_{28}(t)$ is approximately given by $\alpha_0 + 2\,\alpha_1 \times (t - 20\,^\circ\text{C})$ (see equation (6)). In addition to the curve of $\alpha_{28}(t)$ shown in figure 8 (heavy solid line), the overall standard uncertainty, $u(\alpha_{28})$, is displayed as a grey belt. For comparison, the curve of the CTE of $^{\text{nat}}$Si is plotted as a thin line. Considering the measurement uncertainty the difference between the two curves is of significance only in the central region of the temperature interval. At 20 °C the difference corresponds approximately to the uncertainty of α_{28}, which is $u(\alpha_{28}) = 3.0 \times 10^{-9}\,\text{K}^{-1}$ at this temperature.

A difference between the CTEs of ^{28}Si and $^{\text{nat}}$Si was predicted theoretically in [13]. Figure 9 shows the difference of the CTEs as a function of the temperature (dashed line) together with the difference in the experimental results (solid line). At 20 °C both lines agree within approximately $1.7 \times 10^{-9}\,\text{K}^{-1}$, which is well within the experimental uncertainty of $3.0 \times 10^{-9}\,\text{K}^{-1}$. This is also the case in the overall temperature range displayed.

4.2. Results of the measurements at NIST

The recorded x-ray profiles were fitted with theoretical dynamical diffraction profiles to obtain the angular profile

Table 2. Lattice spacing differences between ^{nat}Si and ^{28}Si as a function of temperature.

Data set	Temperature t / °C	$u(t)$/°C	$(d_{28} - d_{nat})/d_{nat} \times 10^6$	$u((d_{28} - d_{nat})/d_{nat}) \times 10^6$
1	21.131	0.026	1.9540	0.0049
2	24.205	0.118	1.9436	0.0056
3	21.147	0.002	1.9557	0.0044

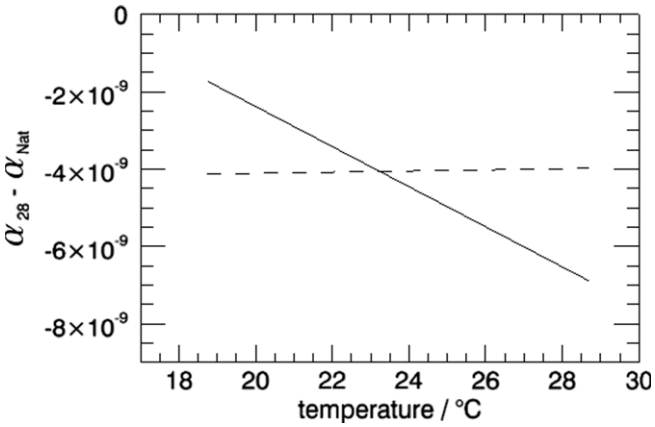

Figure 9. Difference of the CTE of ^{28}Si and ^{nat}Si as a function of the temperature. The dashed line represents the theoretical result and the solid line is based on the experimental results.

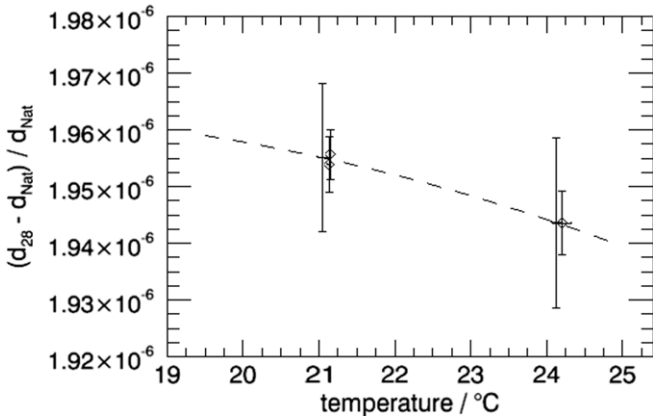

Figure 10. Results of the lattice parameter measurements from section 4.2 (diamond symbols) as a function of temperature. The dashed line indicates the calculated relative difference of the lattice parameters of ^{nat}Si and ^{28}Si based on the experimental result for the CTE of ^{28}Si presented in section 4.1. The two long error bars indicate the uncertainty of the latter curve.

positions. The detailed shapes of the recorded and theoretical dynamical diffraction profiles are sensitive to the thicknesses of the first and second crystal lamellas. In order to obtain the best fits, slightly different theoretical profiles were used for ^{nat}Si and ^{28}Si. The target thickness of the crystal lamellas used on the NIST comparator is 0.455 mm and the inferred difference in thickness between the ^{nat}Si and ^{28}Si crystals to obtain the best fits is 0.010 mm. This small difference is within the tolerance expected from the cutting and etching procedures that are used.

The results of the lattice parameter difference measurements are presented explicitly in table 2 and graphically in figure 10 including uncertainties in both the lattice parameter difference and temperature measurements. The lattice parameter difference uncertainty includes systematic contributions from temperature (3.0×10^{-9}), crystal alignment (1.0×10^{-9}) and precise location of the x-ray beams on the crystals (3.0×10^{-9}). The larger temperature uncertainty at 24.2 °C is likely due to the fact that the room temperature set point was at its maximum value.

4.3. Comparison of the results

Since the concentration of vacancies is low in the crystals used for the Avogadro project [14], a potential difference of the CTE results on the macroscopic and microscopic scale is neglected. Hence, in order to check the results of PTB and NIST for consistency, the result for $\alpha_{28}(t)$ from the optical length measurements was used to calculate the curve of the relative difference of the lattice parameters of ^{nat}Si and ^{28}Si as a function of temperature.

First, the lattice parameters $d_{nat}(22.5\,°C) = 192.015\,5710 \times 10^{-12}$ m [15] and $d_{28}(21.139\,°C) = 192.015\,2742 \times 10^{-12}$ m (calculated from the mean of the data sets 1 and 3 in table 2) of ^{nat}Si and ^{28}Si, respectively, were converted to the reference temperature of 20 °C:

$$d_{nat}(20\,°C) = \frac{d_{nat}(22.5\,°C)}{1 + \alpha_{0,nat} \times (22.5\,°C - 20\,°C) + \alpha_{1,nat} \times (22.5\,°C - 20\,°C)^2},$$

$$d_{28}(20\,°C) = \frac{d_{28}(21.139\,°C)}{1 + \alpha_0 \times (21.139\,°C - 20\,°C) + \alpha_1 \times (21.139\,°C - 20\,°C)^2} \quad (7)$$

with the parameters $\alpha_{0,nat} = 2.5554 \times 10^{-6}\,K^{-1} \pm 0.0002 \times 10^{-6}\,K^{-1}$ and $\alpha_{1,nat} = 4.58 \times 10^{-9}\,K^{-2} \pm 0.04 \times 10^{-9}\,K^{-2}$ published in [16] and with α_0 and α_1 as given in equation (5). The data from [16] are in agreement with those from former measurements of the CTE of ^{nat}Si [17, 18], but have to our knowledge the smallest uncertainty.

Then, in the next step, the expressions

$$d_{nat}(t) = d_{nat}(20\,°C) \times \left(1 + \alpha_{0,nat} \times (t - 20\,°C) + \alpha_{1,nat} \times (t - 20\,°C)^2\right),$$

$$d_{28}(t) = d_{28}(20\,°C) \times \left(1 + \alpha_0 \times (t - 20\,°C) + \alpha_1 \times (t - 20\,°C)^2\right) \quad (8)$$

define the curve of the temperature dependence of the lattice parameters of ^{nat}Si and ^{28}Si, respectively. With equations (8)

one can calculate the behaviour of the relative difference of the lattice parameters

$$\frac{d_{28}(t) - d_{\mathrm{nat}}(t)}{d_{\mathrm{nat}}(t)}$$

dependent on the temperature in order to compare the resulting values with the measurement results of NIST. In figure 10 both the calculated function (dashed line) and the data points (diamond symbols) of the lattice parameter measurements are plotted in the same coordinate system. The data coincide within the given uncertainty range. This finding acts as a validation of the result for the value of the CTE of ^{28}Si.

5. Conclusion

For precise diameter measurements of the Avogadro project's spheres made of a ^{28}Si crystal the knowledge of the thermal expansion behaviour of ^{28}Si is of fundamental importance. In this paper the determination of the CTE of ^{28}Si in a temperature interval from 17.5 °C to 30.0 °C is described. The results are compared with theoretical considerations and with an independent measurement method, all being in agreement within the measurement uncertainty. This fact provides an important confirmation of the measured result for the CTE of ^{28}Si.

In the central region of the temperature interval investigated in the experiments the CTE of ^{28}Si differs significantly from that of $^{\mathrm{nat}}$Si. Even though the uncertainties of the CTEs at 20 °C are approximately equal to the difference in the CTEs at that temperature, the CTE as given by equation (6) should be used for ^{28}Si crystals instead of that for natural silicon.

Disclaimer

The trade name *MATHEMATICA* is included to more completely describe the procedures. Such identification does not suggest endorsement nor indicate that this product is necessarily best suited for this application.

References

[1] Becker P, Bièvre P D, Fujii K, Glaeser M, Inglis B, Luebbig H and Mana G 2007 Considerations on future redefinitions of the kilogram, the mole and of other units *Metrologia* **44** 1–14

[2] Fujii K *et al* 2005 Present state of the Avogadro constant determination from silicon crystals with natural isotopic compositions *IEEE Trans. Instrum. Meas.* **54** 854–9

[3] Becker P *et al* 2006 Large-scale production of highly enriched ^{28}Si for the precise determination of the Avogadro constant *Meas. Sci. Technol.* **17** 1854–60

[4] Nicolaus R A and Bönsch G 2005 Absolute volume determination of a silicon sphere with the spherical interferometer of PTB *Metrologia* **42** 24–31

[5] Nicolaus R A and Geckeler R D 2007 Improving the measurement of the diameter of Si-spheres *IEEE Trans. Instrum. Meas.* **56** 517–22

[6] Preston-Thomas H 1990 The international temperature scale of 1990 (ITS-90) *Metrologia* **27** 3–10

[7] James J D, Spittle J A, Brown S G R and Evans R W 2001 A review of measurement techniques for the thermal expansion coefficient of metals and alloys at elevated temperatures *Meas. Sci. Technol.* **12** R1–15

[8] Schödel R 2008 Ultra high accuracy thermal expansion measurements with PTB's precision interferometer *Meas. Sci. Technol.* **19** 084003

[9] ISO 1993 *Guide to the Expression of Uncertainty in Measurement* 1st edn (Geneva: International Organisation for Standardisation) (corrected and reprinted 1995)

[10] Schödel R 2005 Accurate extraction of thermal expansion coefficients and their uncertainties from high precision interferometric length measurements *Proc. SPIE* **5879** 587901

[11] Kessler E G, Henins A, Deslattes R D, Nielsen L and Arif M 1994 Precision comparison of the lattice parameters of silicon monocrystals *J. Res. Natl Inst. Stand. Technol.* **99** 1–18
Kessler E G, Henins A, Deslattes R D, Nielsen L and Arif M 1994 *J. Res. Natl Inst. Stand. Technol.* **99** 285 (erratum)

[12] Hanke M and Kessler E G 2005 Precise lattice parameter comparison of highly perfect silicon crystals *J. Phys. D: Appl. Phys.* **38** A117–20

[13] Zhernov A P 2000 Lattice constant and coefficient of linear thermal expansion of the silicon crystal. Influence of isotopic composition *Low Temp. Phys.* **26** 908–15

[14] Gebauer J, Rudolf F, Polity A, Krause-Rehberg R, Martin J and Becker P 1999 On the sensitivity limit of positron annihilation: detection of vacancies in as-grown silicon *Appl. Phys.* A **68** 411–6

[15] Becker P, Cavagnero G, Kütgens U, Mana G and Massa E 2007 Confirmation of the INRiM and PTB determinations of the Si lattice parameter *IEEE Trans. Instrum. Meas.* **56** 230–4

[16] Schödel R and Bönsch G 2001 Precise interferometric measurements at single crystal silicon yielding thermal expansion coefficients from 12 °C to 28 °C and compressibility *Recent Development in Traceble Dimensional Measurements* ed J E Decker and N Brown *Proc. SPIE* **4401** 54–62

[17] Okaji M and Imai H 1992 Development of an interferometric dilatometer with optical heterodyne system *Netsu Bussei* **6** 83–8

[18] Lyon K G, Salinger G L, Swenson C A and White G K 1977 Linear thermal expansion measurements on silicon from 6 to 340 K *J. Appl. Phys.* **48** 865–8